I. WAVES

Jonathan GULA
gula@univ-brest.fr

I. WAVES

I.1. Introduction

I.2. General properties of Waves

I.3. Different type of ocean waves

I.3.1 Surface Gravity Waves

I.3.2 Internal Waves

I.3.3 Acoustic Waves

I.4. Group speed and Ray Theory

I.4.1 Group Speed

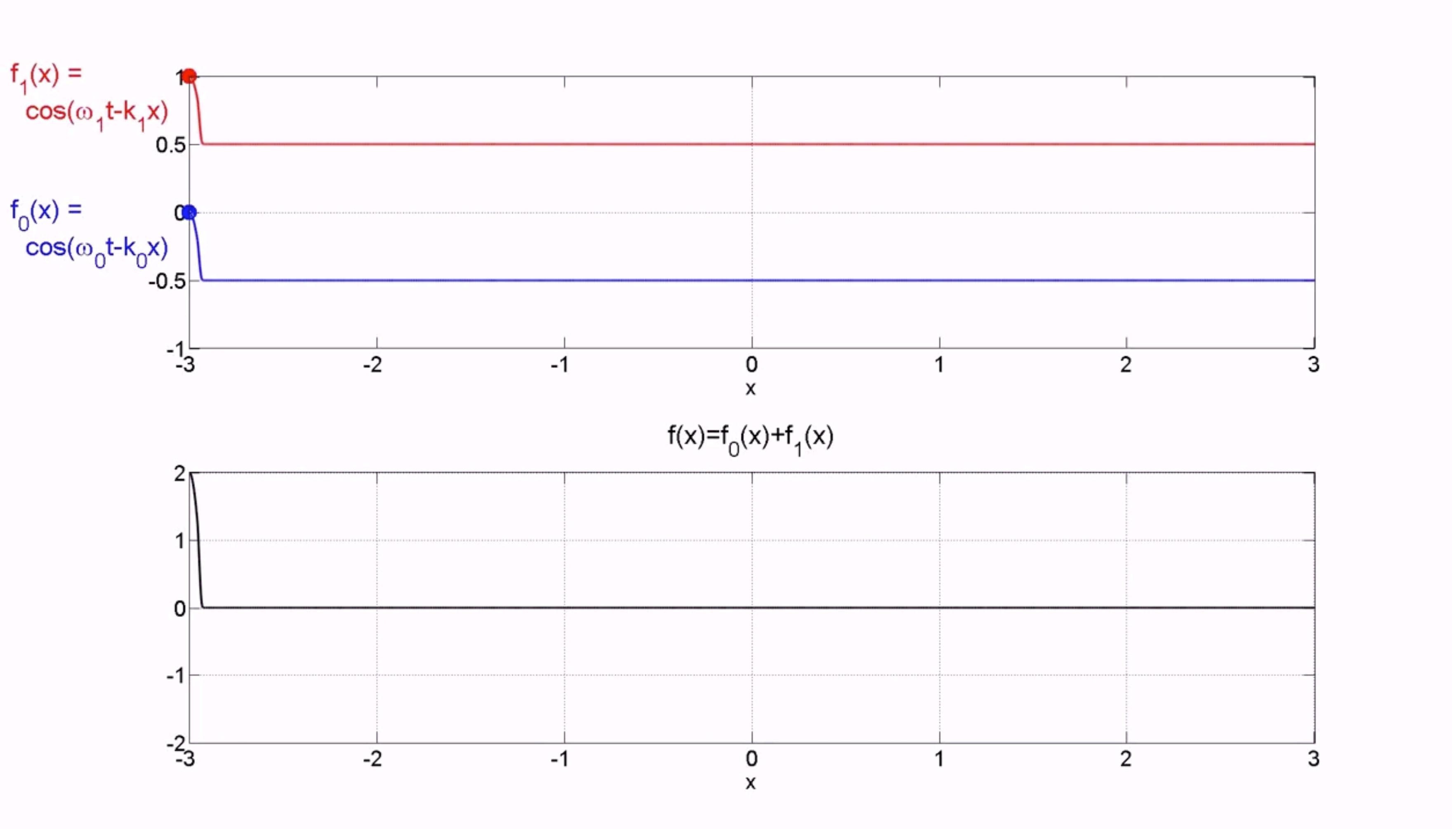

Internal Waves

Observation of an internal wave attractor in a confined, stably stratified fluid

Leo R. M. Maas*, Dominique Benielli†, Joël Sommeria† & Frans-Peter A. Lam*

* *Netherlands Institute for Sea Research, PO Box 59, 1790 AB Texel, The Netherlands*

† *Ecole Normale et Superieure de Lyon, Laboratoire de Physique, 46 allée d'Italie, 69364 Lyon cedex 07, France*

NATURE | VOL 388 | 7 AUGUST 1997

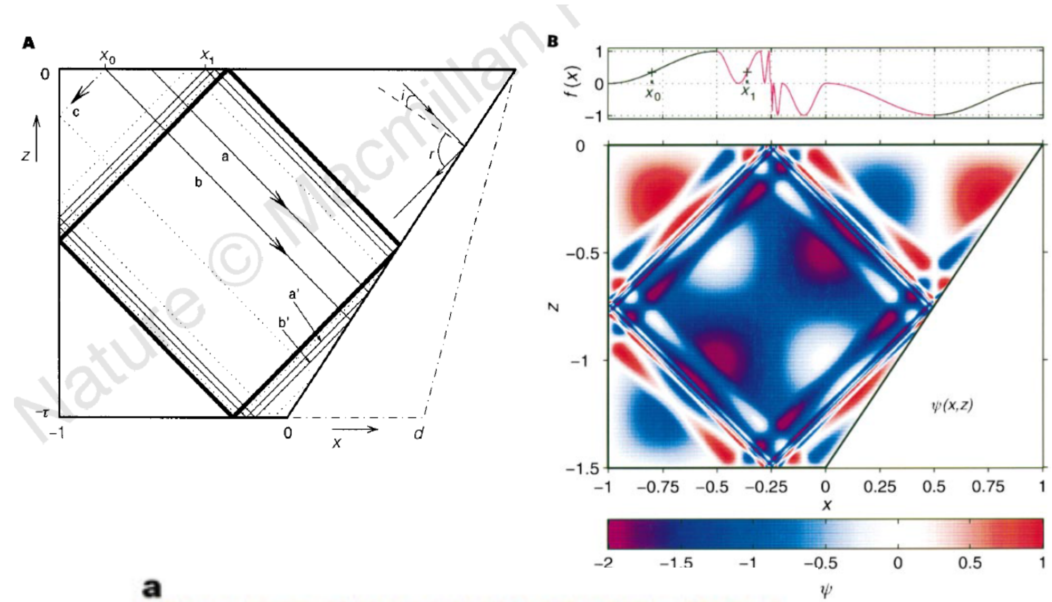

a

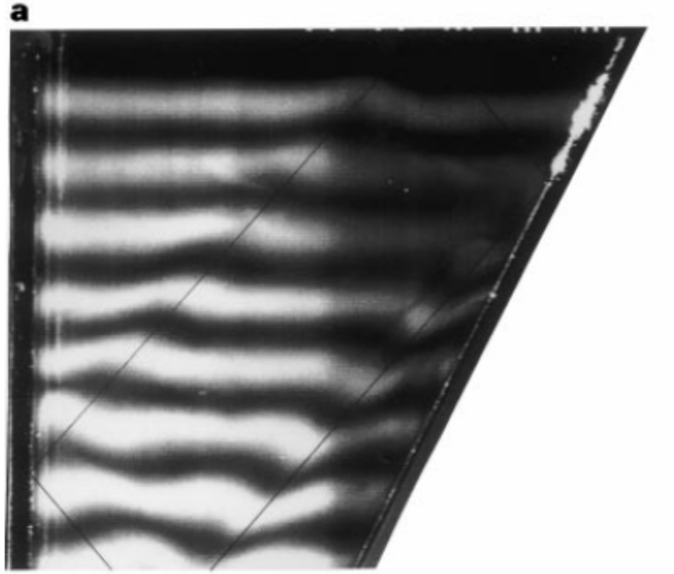

a

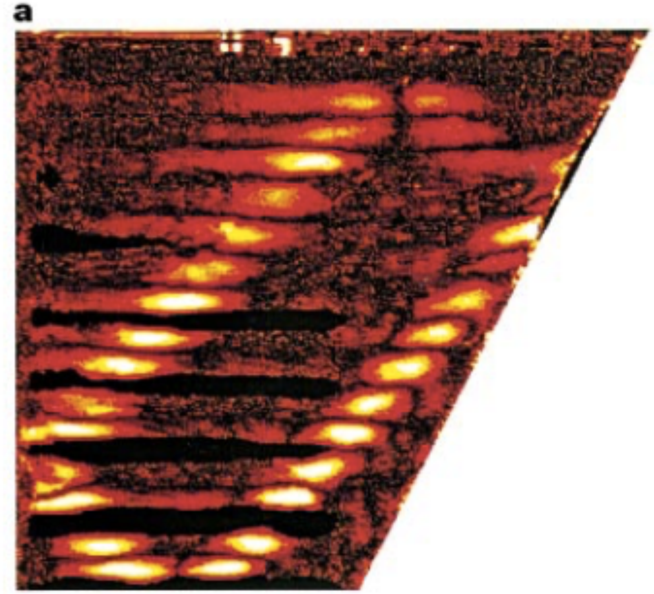

Internal Waves

- For a linear N(z):

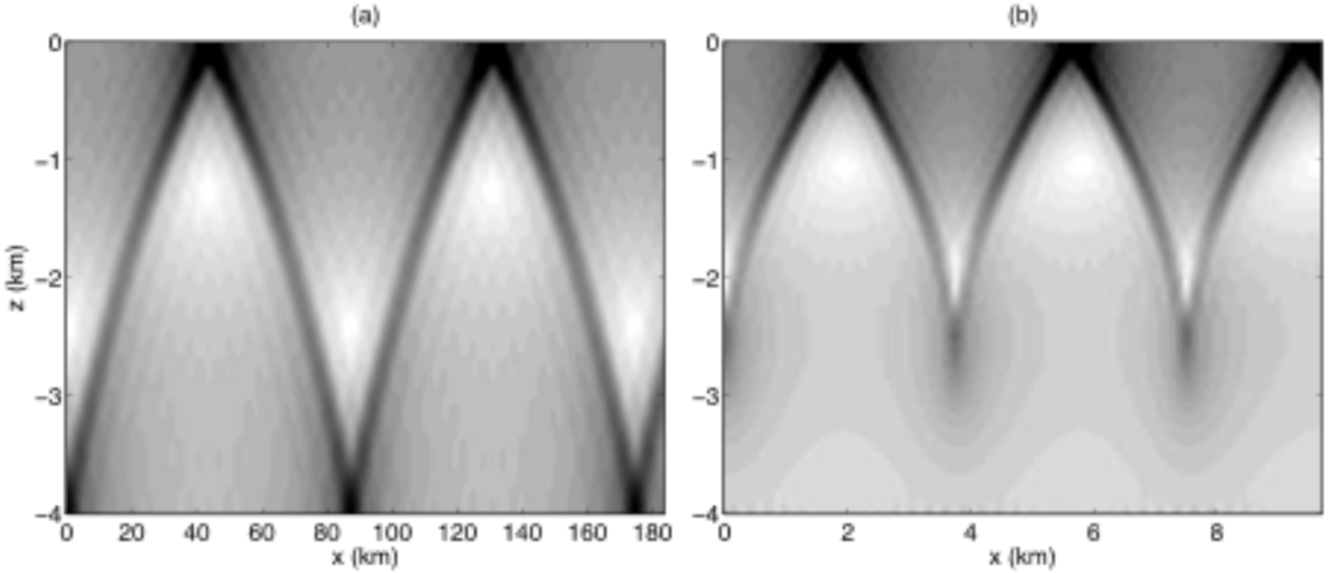

Fig. 5.16: Solution for a linearly varying $N(z)$; the amplitude of u is shown for a superposition 15 modes, with modal coefficients $a(n) = 1/n$. White denotes zero; black, maximum values. In **a**, internal-wave beams can propagate at any depth, but are refracted due to the decrease of N with depth. In **b**, a higher wave frequency is chosen, such that $|f| < N < \omega$ in the deeper part of the water column; hence, internal waves are trapped in the upper layer.

Internal Waves

Internal tidal beams:

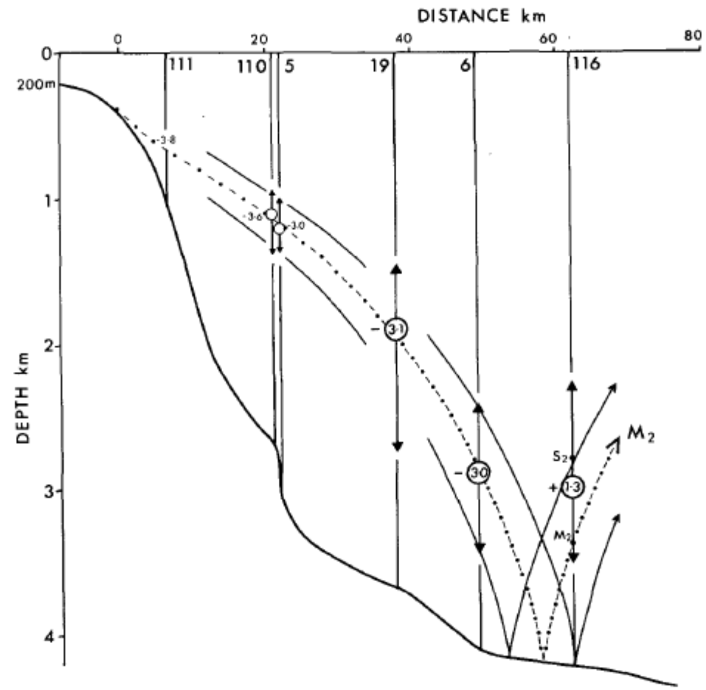

FIG. 9. Diagram showing the theoretical ray path (chained line) for a beam of internal tidal energy at the M_2 tidal frequency emanating from the critical depth (385 m) on the upper slopes and reflecting off the Biscay abyssal plain at a depth of about 4200 m, 58 km from the critical point. Also shown is a summary of the internal tidal oscillations obtained during the RRS *Challenger* cruises in 1988 (CH 31/88) and 1987 (CH 18/87). Vertical lines represent mooring and CTD station positions and are identified with numbers. CTD stations 5 and 6 and mooring 116 are from the 1988 cruise, whereas moorings 110 and 111 and CTD 19 were obtained in 1987. The depth of the maximum amplitude of the internal tidal oscillation found at each station is plotted as an open circle and the range where the amplitude is more than 70% of the maximum value is indicated by the arrows. Two further rays are shown (solid lines) passing through the 70% limits near mooring 110. The phase of the maximum upward displacement is given (within the circles) in hours with respect to HWP. A ray at the M_2 tidal frequency would intersect mooring 116 at the depth marked M_2; S_2 is the corresponding point for a ray at the S_2 tidal frequency. The topography is depicted by the bold line and is critical at 385 m; the horizontal distance scale is measured from the critical point.

Internal Waves

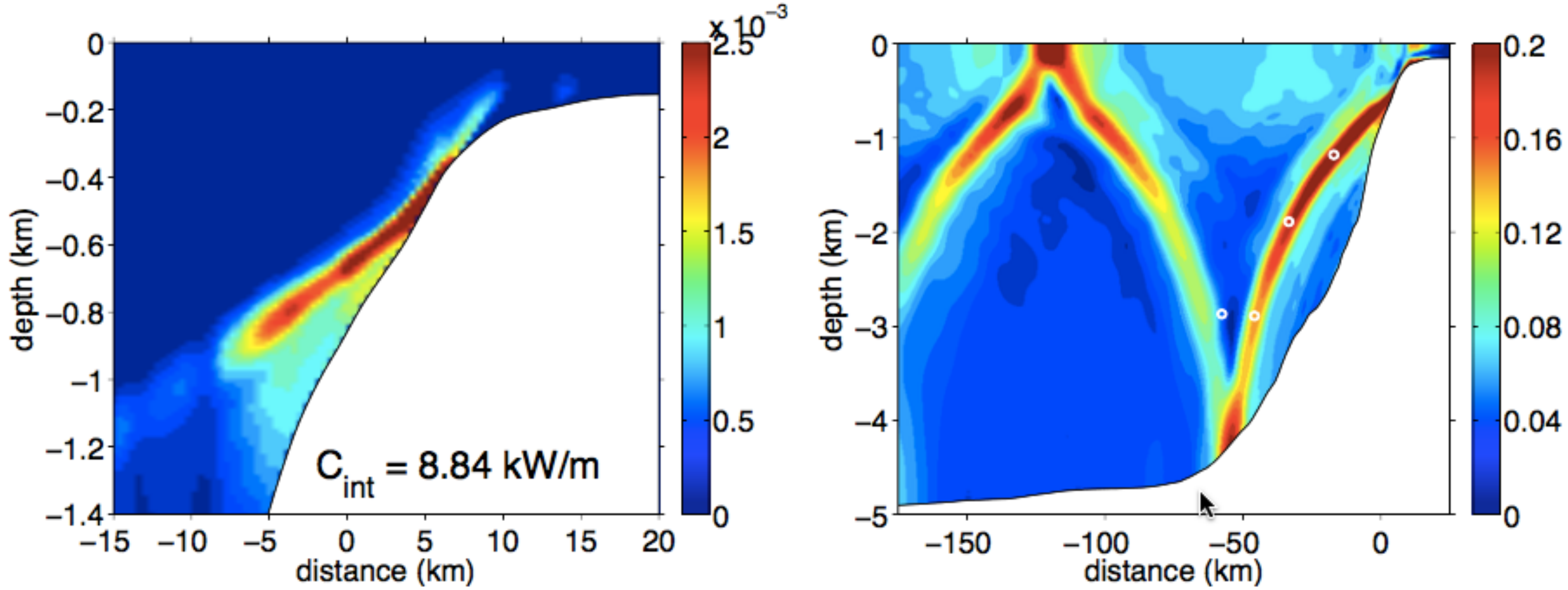

Results from a numerical model, here applied to the Bay of Biscay. Left: The spatial distribution tidally-averaged conversion rate, $C = -\rho_* \langle bW \rangle$, in W/m3; Right: The internal tide emanating from the continental slope, here depicted in terms of the amplitude of the cross-slope velocity u, in m/s.

Internal Waves

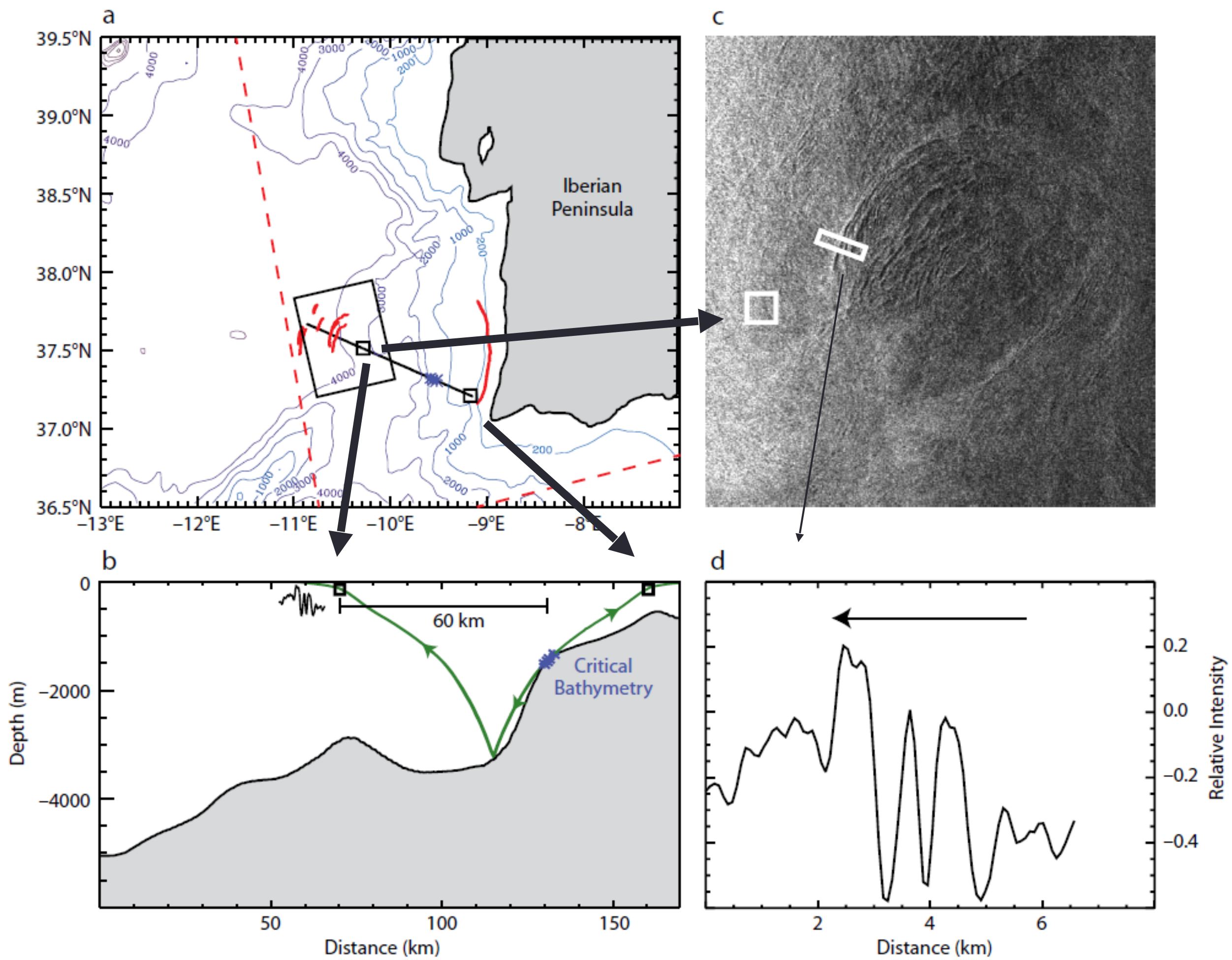

Figure 5. (a) Map of area southwest of the Iberian Peninsula with internal solitary wave crests marked in red based on one Envisat Advanced Synthetic Aperture Radar (ASAR) image in Wide-Swath Mode dated August 4, 2004 (22:27 UTC). (b) Ray-tracing diagram showing internal tide ray paths (in green; emanating from critical topography, in blue) along the black line in part (a). The small black squares in part (a) show where the ray path crosses the near-surface thermocline (taken at a depth of 50 m), and are also marked in part (b). (c) Full-resolution detail of a nonlinear internal wave train observed to propagate toward the west-northwest and believed to be generated by the tidal beam in part (b). (d) Radar backscatter profile showing the wavelength cross section of a nonlinear internal wave train generated by the tidal beam. The narrow rectangle in part (c) represents the cross section from which part (d) was obtained. The square in part (c) is a background backscatter reference used to normalize the radar profile in part (d). Zero in part (d) represents the average unperturbed backscatter of the SAR image in part (c).

Internal Waves in a sheared flow

- Negative angle: $$\theta_e < 0$$

  The ray is bent towards the normal to the current

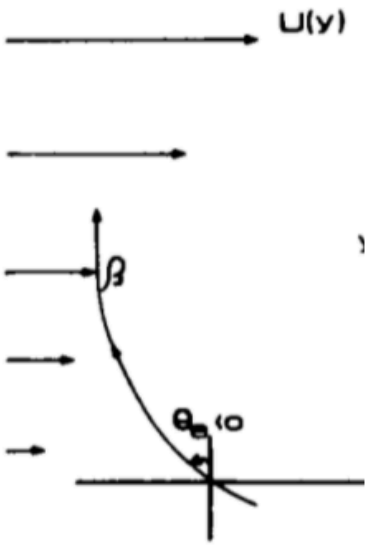

- Internal reflection:

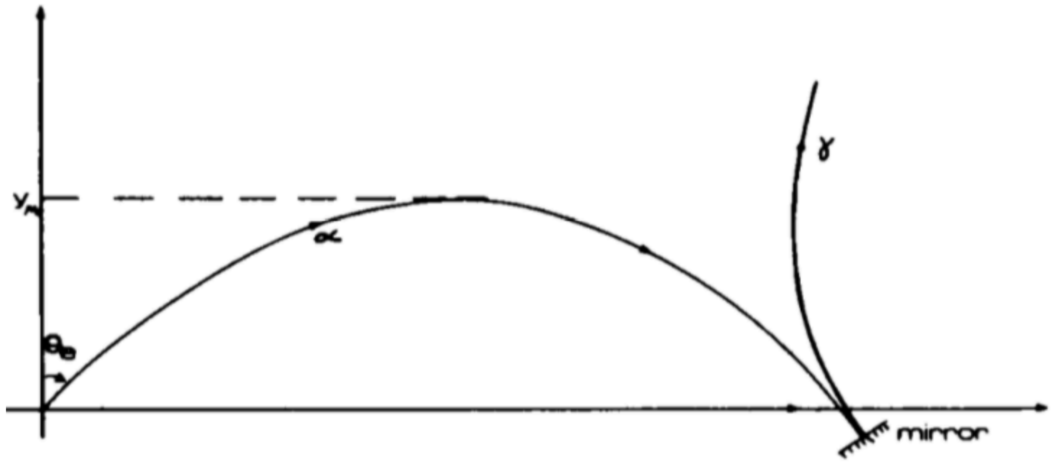

Internal Waves and critical layers

A critical layer is a region where the velocity of the flow is equal to the phase speed of the waves **[Bretherton & Garrett, 1968]**

$$\omega = \vec{k} \cdot \vec{U}$$

At such level, energy is transferred to the mean flow and turbulence is generated.

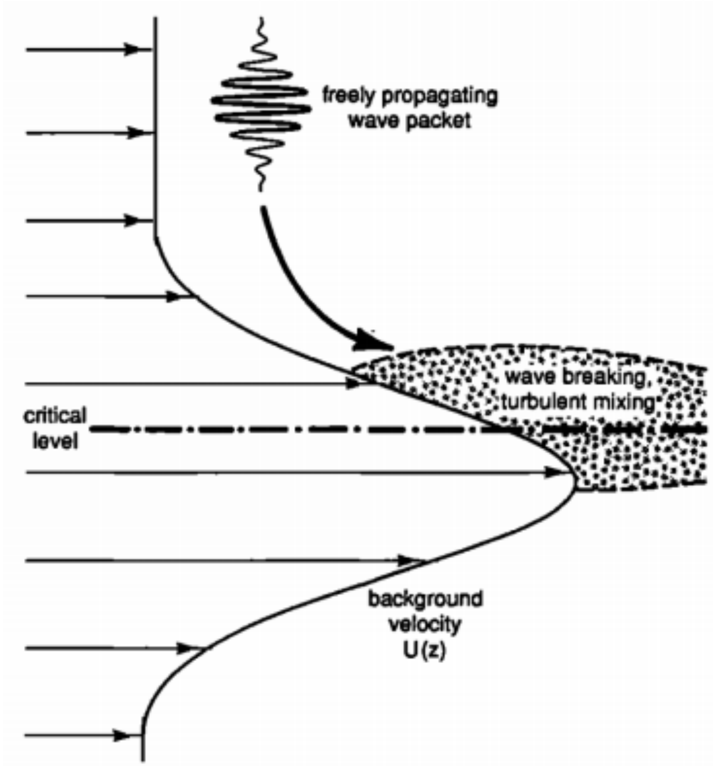

(See LeBlond & Mysak, p 387)

[Winters & D'Asaro, 1989, 1995]

Internal Waves and critical layers

- For small wave in a presence of a vertical shear: If the background flow increases as a small wave approaches, it is stretched and rotated due to the shear until it's group velocity is nearly horizontal, wavelength increases infinitely, lending the wave's energy to the background.

- For large amplitude waves, the steepness of the wave causes breaking before absorption occurs.

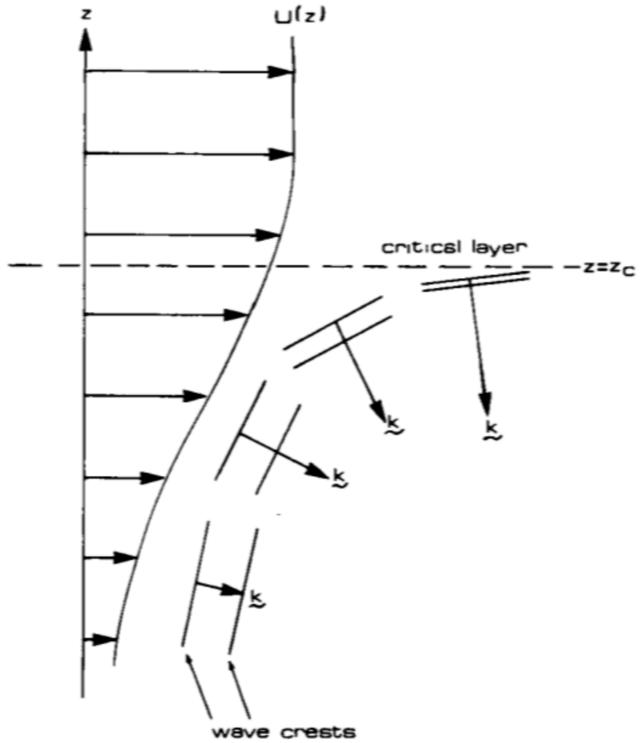

[LeBlond & Misak]

Internal Waves and critical layers

- Short internal Lee waves have a high probability of encountering critical layers and be absorbed in the lower 1 km above ocean bottom:

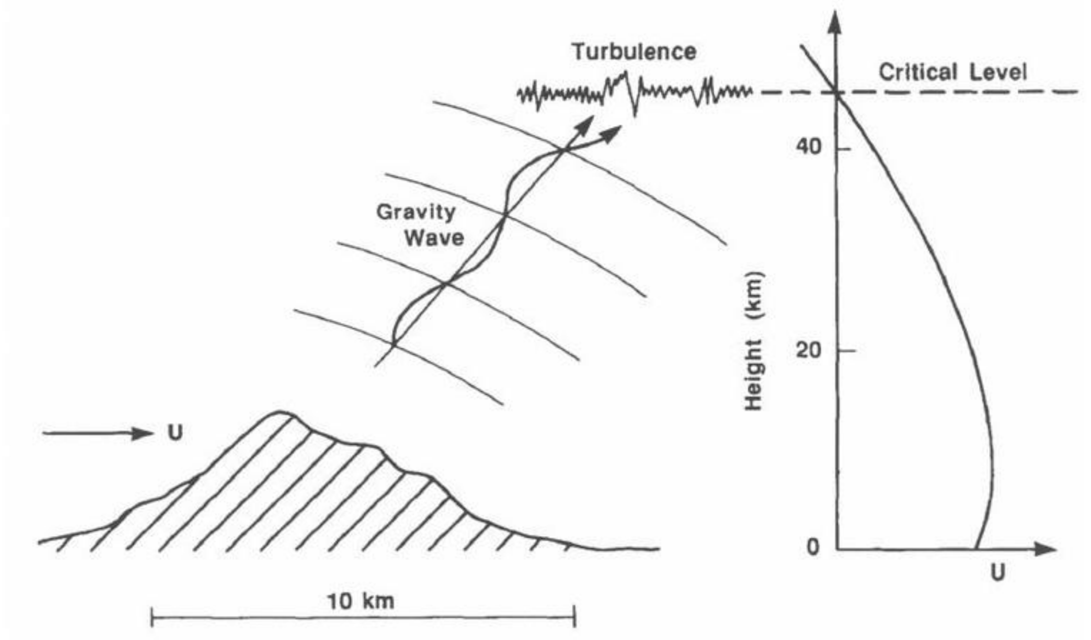

Acoustic Waves

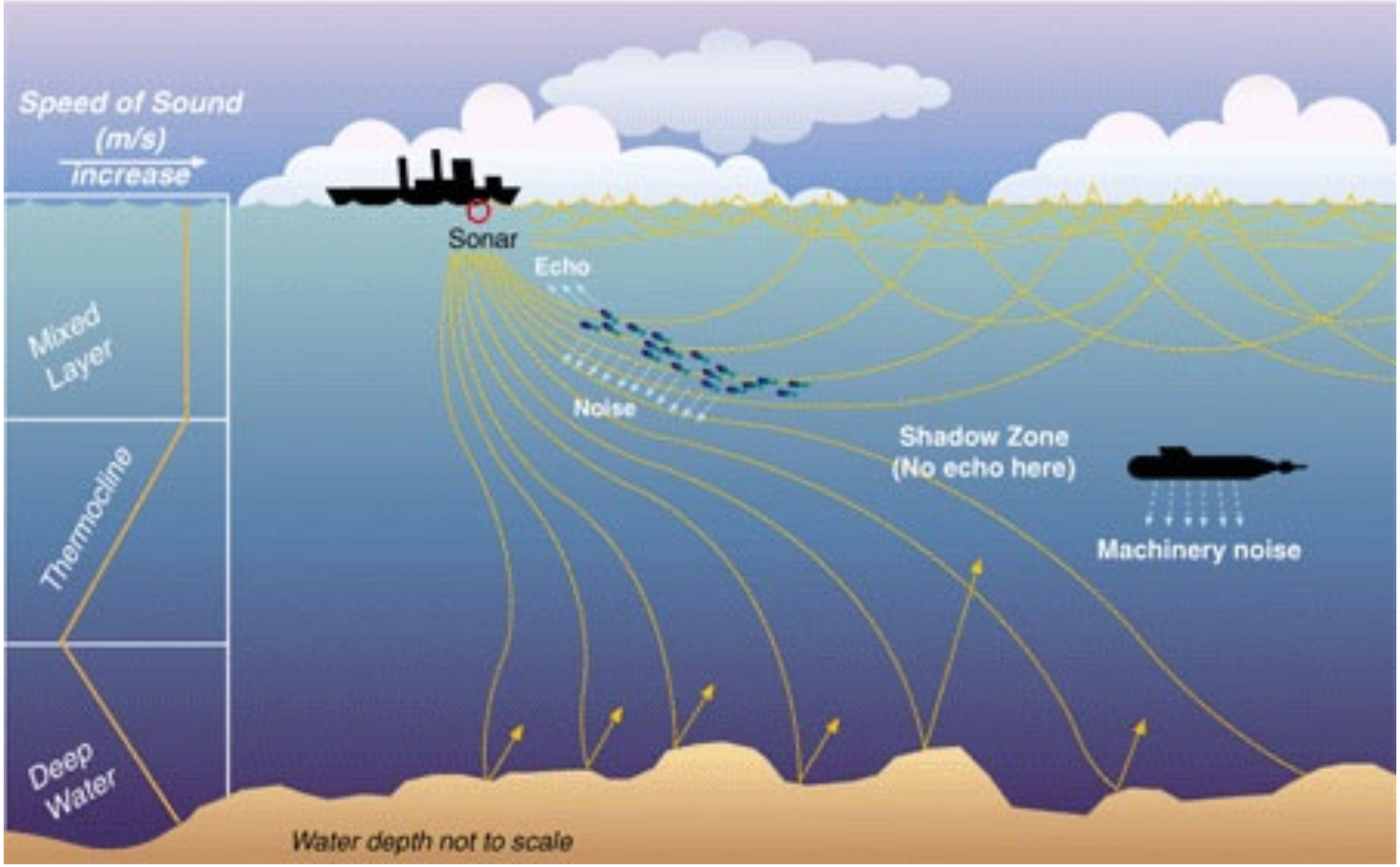

I.4.2 Ray Theory

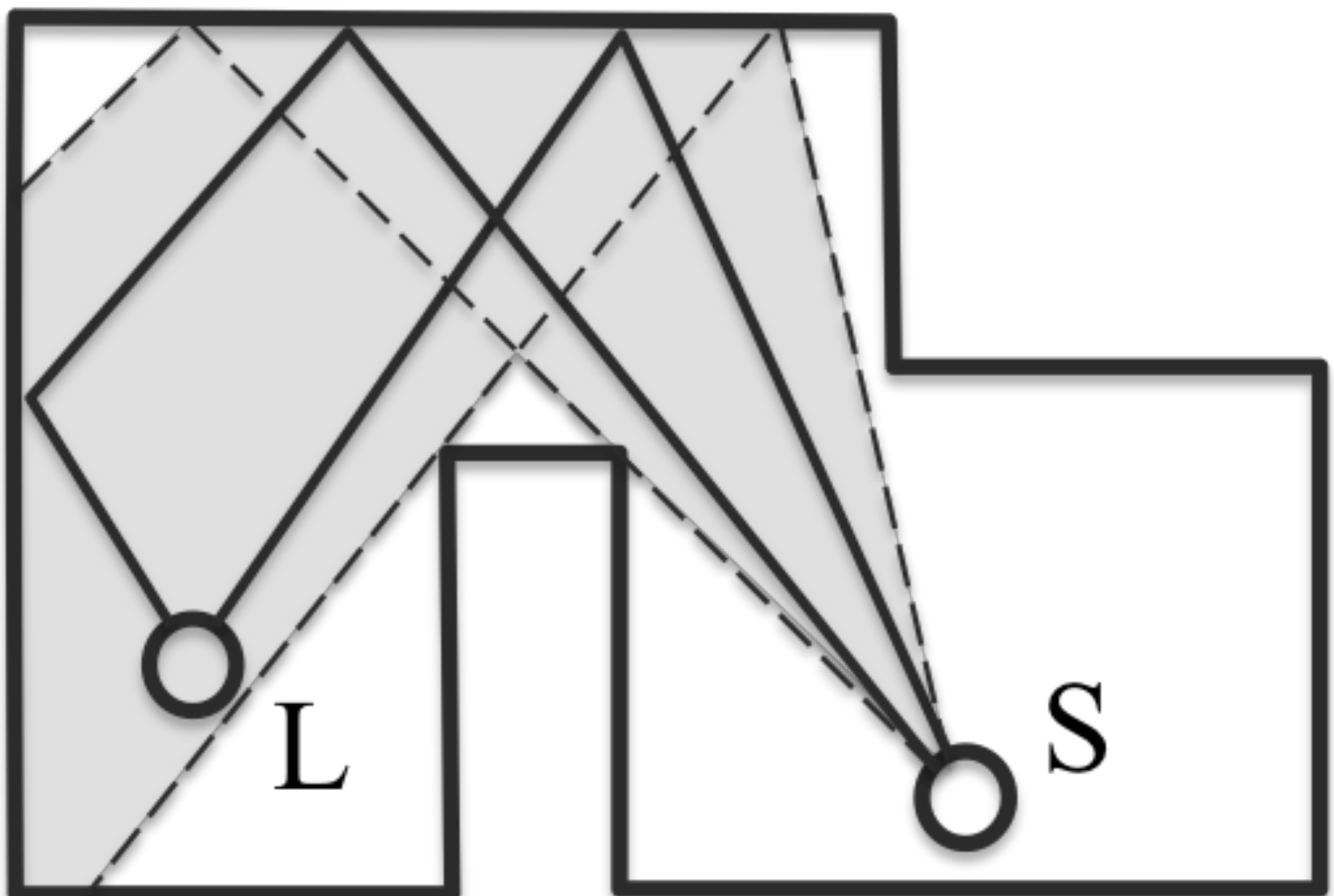

I.4.2 Ray Theory

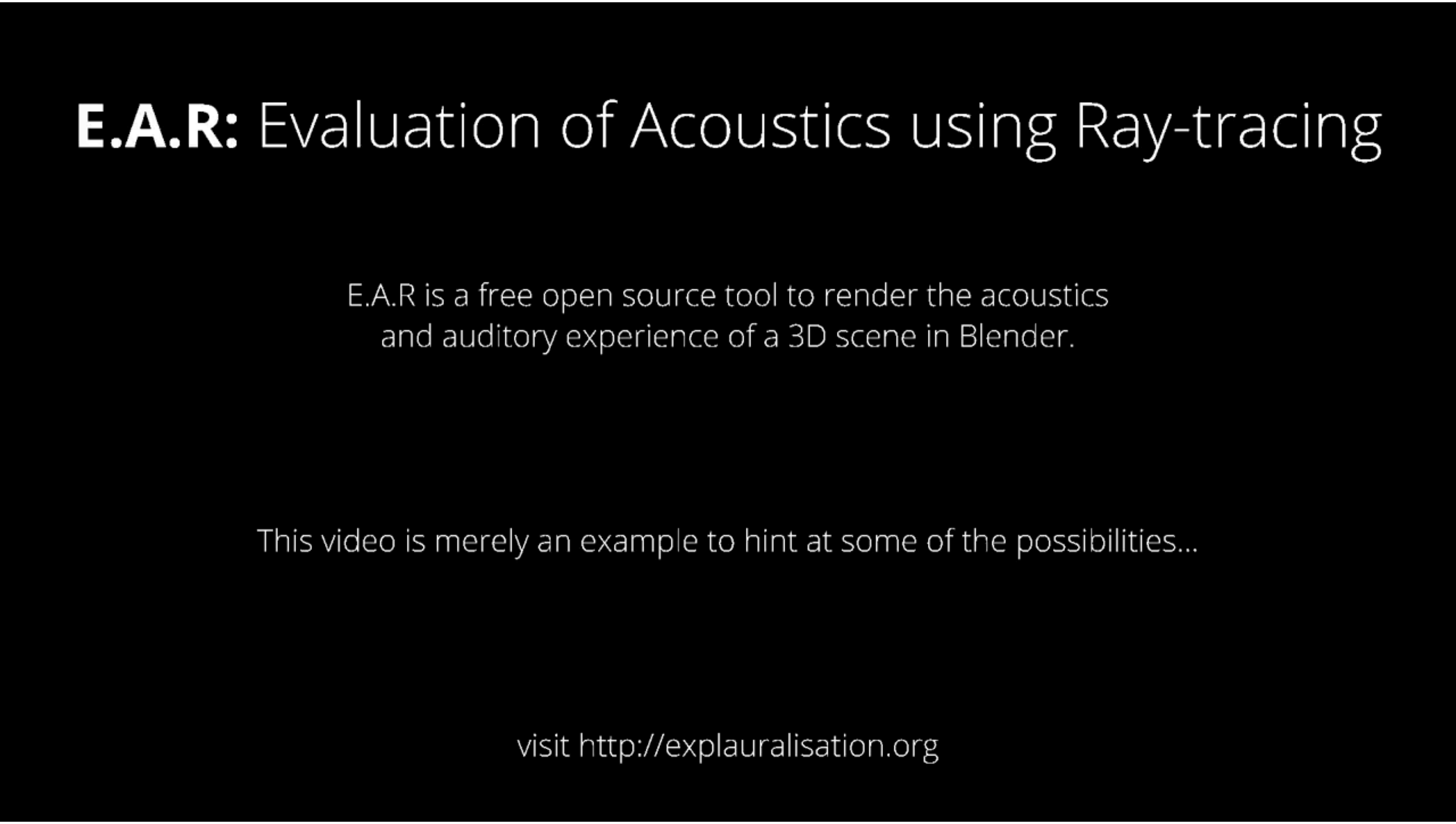

I.4.2 Ray Theory

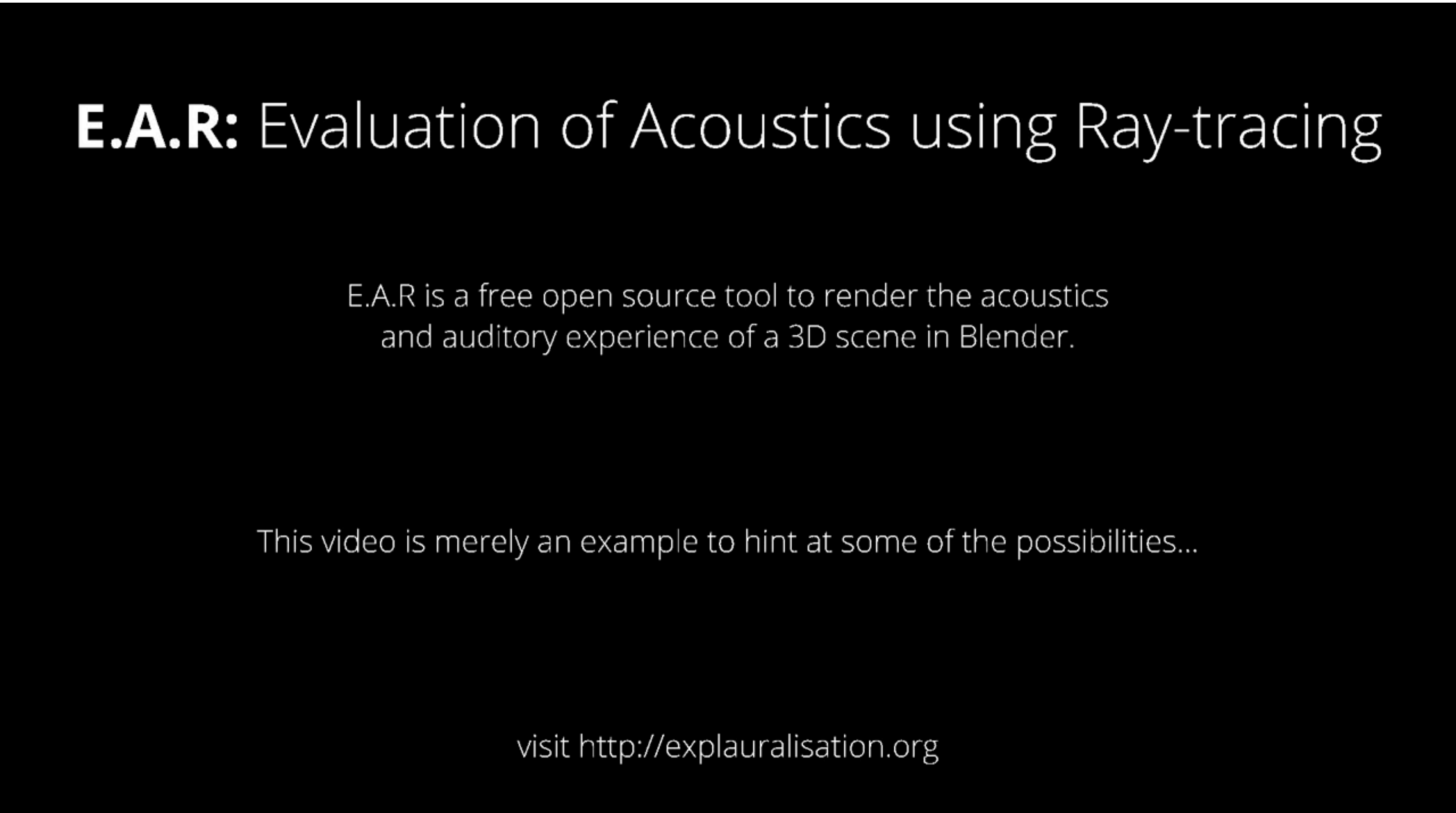

I.4.2 Ray Theory

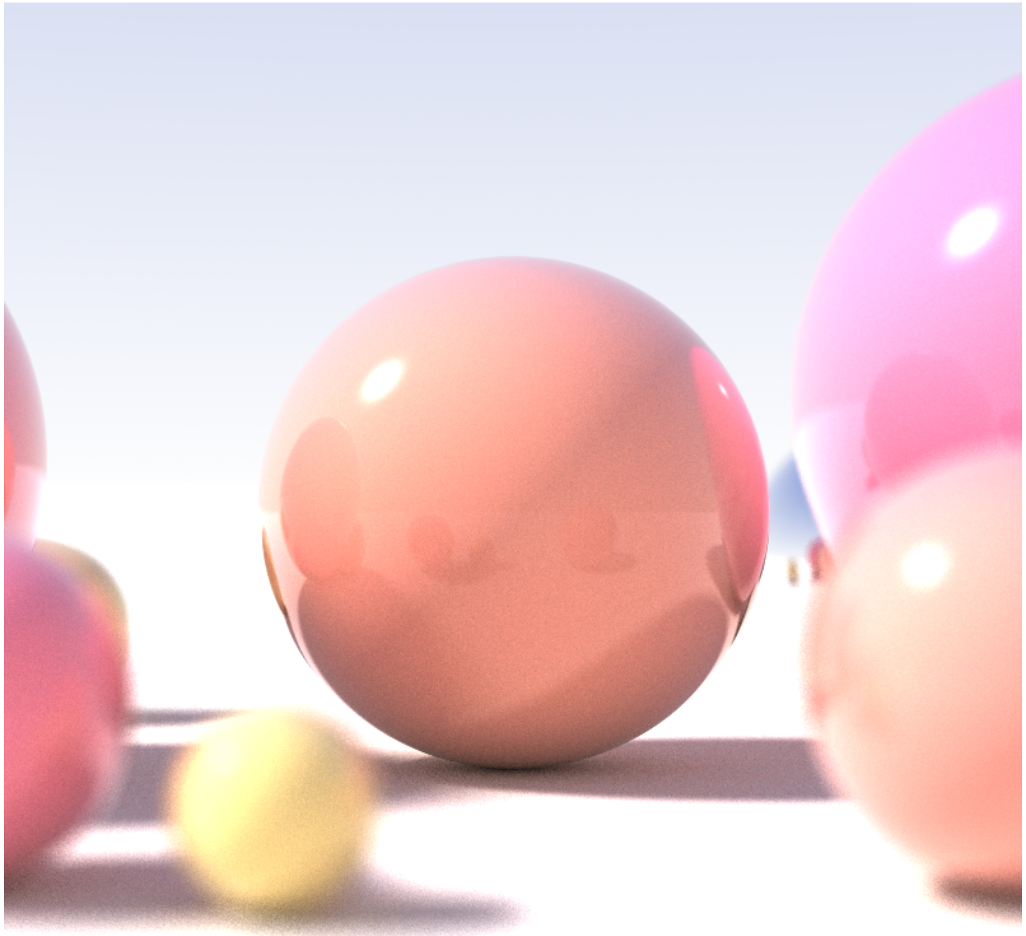

I.4.2 Ray Theory

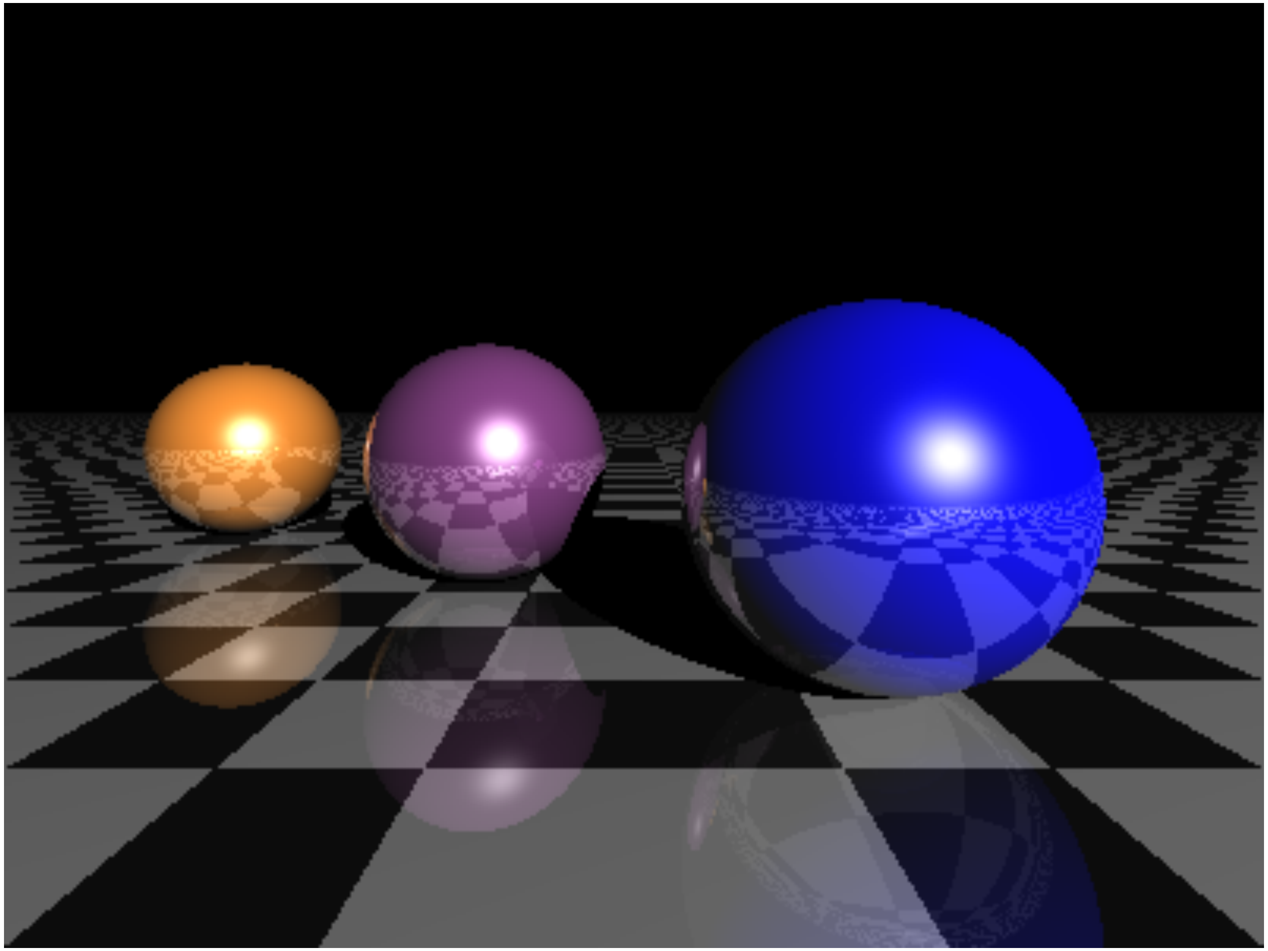

https://gist.github.com/rossant/6046463